IEEE Access
Multidisciplinary | Rapid Review | Open Access Journal

Received April 13, 2019, accepted May 19, 2019, date of publication May 24, 2019, date of current version June 10, 2019.

Digital Object Identifier 10.1109/ACCESS.2019.2918785

Changes in Binocular Color Fusion Limit Caused by Different Disparities

ZAIQING CHEN[1,2], YONGHANG TAI[2], JUNSHENG SHI[2], JUN ZHANG[2], XIAOQIAO HUANG[2], AND LIJUN YUN[1]

[1]School of Information Science and Technology, Yunnan Normal University, Kunming 650500, China
[2]Yunnan Key Laboratory of Optoelectronic Information Technology, Kunming 650500, China

Corresponding authors: Yonghang Tai (taiyonghang@126.com) and Junsheng Shi (shi-js@263.net)

This work was supported in part by the National Science Foundation of China under Grant 61865015, Grant 61875171, and Grant 61741516, and in part by the Key Program of the Yunnan Education Commission of China under Grant 2018FA033.

ABSTRACT When the color asymmetry between the left and right eyes exceeds a threshold value, named binocular color fusion limit, the color rivalry is said to occur. For stereoscopic displays, the horizontal disparity is the most important information to produce depth perception. When the stereo pair stimuli are presented separately to both eyes with disparities and those two stimuli also differ in color but share an iso-luminance polarity, it is possible for stereopsis and color rivalry to coexist. In this paper, we conducted a psychophysical experiment to quantitatively measure the color fusion limit at different disparity levels. In particular, it examined how disparities affect the binocular color fusion limit. A binocular color fusion limit was measured at five relative disparity levels: 0, ±60, and ±120 arc minutes for five sample color points, which were selected from the 1976 CIE u'v' chromaticity diagram. The experimental results show that the color fusion limit for each sample point varies with the disparity magnitude, disparity sign, and color direction. It is new research finding that the color fusion limit increases as the disparity increases from −120 to +120 arc minutes. The average color fusion limit ranges from 0.036 to 0.064 in terms of Euclidean distance in the u'v' chromaticity diagram ($\Delta E_{u'v'}$). The new finding shows that the human eye has different information processing mechanisms for crossed disparity (sign −) and uncrossed disparity (sign +), and uncrossed disparity can contribute to color fusion. We suggest that the color fusion limit varies with the color direction, but it has nothing to do with the distribution of cone cells. The color fusion limit was quantified by using ellipses in the chromaticity diagram, and the axis of the ellipses ranges from 0.017 to 0.145 $\Delta E_{u'v'}$. The experiments and data analysis in this paper indicate that the binocular disparity fusion affects binocular color fusion. This research result can strongly support 3D system design and 3D content creation.

INDEX TERMS 3D displays, color fusion limit, color measurement, color vision, stereo vision, visual comfort.

I. INTRODUCTION

When one image is presented to one eye and a very slightly different image is presented to the other (also known as dichoptic presentation), the brain can fuse these two images into a single perception and yield stereopsis. The spatial differences between the two retinal images called binocular disparities [1], which can be used to recover the three-dimensional (3D) aspects of a scene. Stereoscopic 3D displays are the devices to implement these disparity cues, which have gained momentum in terms of research and commercial successes recently [2], [3]. However, current 3D technologies can provide several potential sources of binocular mismatches in shape, brightness, and color [4]. Those mismatches are unpleasant and annoying for 3D display systems, which may result from optical differences between stereoscopic camera lenses, coding and transmission (compression), multiple views rendering and display type. To address color mismatch, it is an interesting research question that how much color difference can be permitted before the fusion ceases. In literature, the level of color asymmetry between left and right eyes should not exceed a threshold value, known as the binocular color fusion limit [5]. Otherwise, the color rivalry is said to occur, during which

The associate editor coordinating the review of this manuscript and approving it for publication was Sudhakar Radhakrishnan.

one can perceive only one of the two colors and the perception alternates periodically in either the spatial or temporal domain [6]–[8].

It is important to determine the binocular color fusion limit within which the color fusion is assured. This is a basic requirement in creating 3D contents and designing 3D systems. Some researchers have studied the effect of hue or wavelength differences on color rivalry using stimuli of various sizes, intensities, and saturation [9]–[12]. However, there is not sufficient research on quantitative investigations. Previous investigations concentrated on measurements of color fusion limits could be divided into three branches: (1) quantitative measurement for the limit of wavelength (spectral colors); (2) quantitative measurement for the limit of non-spectral colors; and (3) changes in color fusion limit caused by different conditions.

For the limit of spectral colors, Ikeda et al. started to quantify the binocular color fusion limit $\Delta\lambda$ as a function of the wavelength λ [5]. They performed experiments to measure the color fusion limit for seventeen wavelengths covering the range from 500 to 660 nm in about 10 nm steps. Their results showed that the color fusion limit varied from about 10 to 50 nm depending upon the wavelength region investigated. Later Ikeda and Nakashima expanded the measurement into short and long wavelength regions so that the general and accurate properties of the $\Delta\lambda/\lambda$ function could be grasped [13]. The experimental results showed that the limit varied from 15 nm to l00 nm depending upon the wavelength employed with two minima, and the function exhibited a saw wave shape of $\Delta\lambda/\lambda$ curve when the limits were plotted along the spectrum. For the limit of non-spectral colors, Ikeda et al. also obtained the limit for a pair made up of white light and a colored light that varied in purity [5]. They reported that the limits were much too large to compare with the color discrimination limits. A circle with its center at the white light was drawn to fit the limits. In 2011, Jung et al. extended the work and performed experiments to measure the color fusion limit for eight chromaticity points sampled from the CIE 1976 chromaticity diagram at a brightness level of 10 cd/m^2 [14]. The experimental results showed the color fusion limit represented in terms of the Euclidean distance along straight lines in u′ v′ chromaticity diagram ($\Delta E_{u'v'}$), and the color fusion limit was quantified by ellipses in the chromaticity diagram. They reported that the semi-minor axis of the ellipses ranged from 0.0415 to 0.0923 $\Delta E_{u'v'}$ and the semi-major axis ranged from 0.0640 to 0.1560 $\Delta E_{u'v'}$. For changes in color fusion limit caused by different conditions, Qin et al. measured the wavelength difference limit under different brightness levels [15]. Results showed that the shapes of the $\Delta\lambda/\lambda$ function were very similar to Ikeda et al.'s results. They suggested that the range of binocular color fusion limit was less than 10∼80 nm and the limit became smaller with the increase of the brightness of the stimulus. In another study, Qin et al. reported that peripheral visual field could influence the color fusion limit, and the limit of central vision was smaller than the limit of peripheral vision with the same stimuli and the same experimental condition [16]. In 2009, Qin et al. examined the effects of luminance and size of stimuli upon the binocular fusion limit [17]. They measured the binocular color fusion limits $\Delta\lambda$ for each dominant wavelength λ quantitatively with different luminance. Results confirmed the previous Qin's finding [15] that the color fusion limit decreased as the luminance of stimuli increased. Furthermore, they adjusted the visual size of stimuli from 2° to 10° and found that color fusion was more difficult to achieve at 10° than at 2°.

Quantitative investigations are lacking that establish the color fusion limit under different disparity levels. Compared to conventional 2D counterparts, the disparity is the most important information brought by 3D displays, which make one produce the depth perception (stereopsis). Unfortunately, the color mismatch is a common phenomenon in the 3D display system [18], which can cause visual fatigue or visual discomfort when looking at stereoscopic displays [19], [20]. However, it is possible for stereopsis and color rivalry to coexist when a common stimulus is shown to both eyes with disparity and those two monocular stimuli differ only in color but share an iso-luminance polarity. In other words, iso-luminance information allows for fusion and stereopsis [21], [22], while the discrepant color component allows for the rivalry. The visual discomfort has always been described as the number one health issue for the application and development of 3D industry [23], [24]. It should not be ignored that 3D content creation and 3D system design could be seriously affected if the binocular color fusion limit varies with the disparity. Therefore, quantitative measurements of the color fusion limit for disparities can provide valuable guidance for 3D display manufacturers to control the color asymmetry in a safe range.

In a previous work [25], we experimentally measured the binocular color fusion limit for a sample color point which was selected from the 1976 CIE u'v' chromaticity diagram. The preliminary results showed that the fusion limit for the sample point varied with the level and sign of disparity. In this paper, we expand the work to quantify the color fusion limit for five sample color points at five different disparity levels. We intend to discover the relationship between the color fusion limit and the disparity. Furthermore, we collect and analyze the real-world data through well-designed experiments, which can be used in the design of 3D systems and creation of 3D contents. In Section 2, we describe the experimental method, and experimental results and discussions are presented in section 3. Section 4 concludes this paper.

II. METHOD

A. APPARATUS AND VIEWING CONDITIONS

To enable accurate control of color, a calibrated cathode-ray tube (CRT) color monitor (SONY G520) was employed to present experimental stimuli. The monitor connected to a graphics card housed in a personal computer (Intel Core^{TM}2 Duo CPU with 3 GHz processing speed, 4 GB RAM, Microsoft Windows 7) and had a resolution

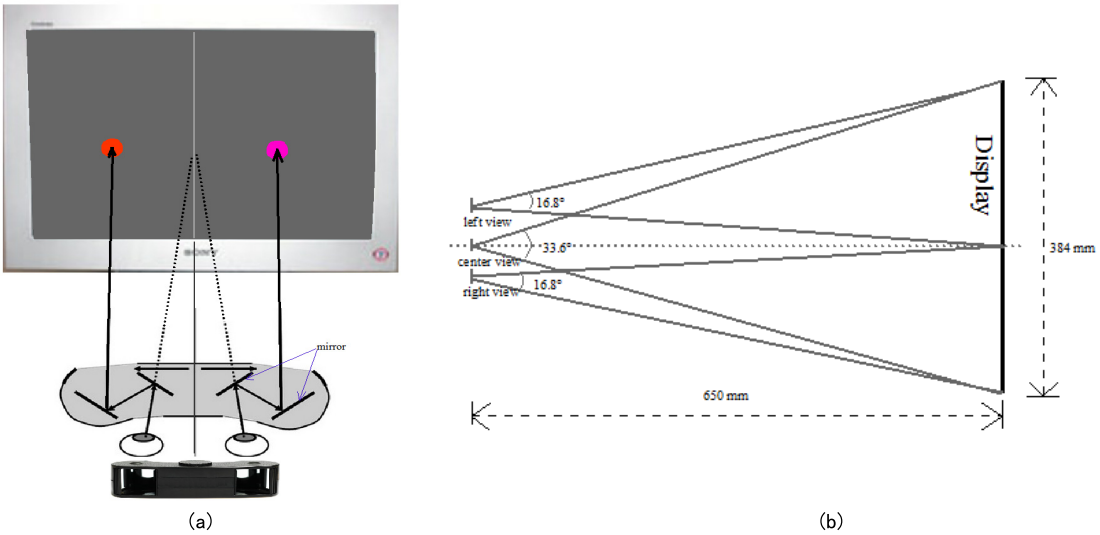

FIGURE 1. Viewing conditions in our experiments. (a) 3D viewing apparatus with a custom-built 4-mirror stereoscope; (b) side by side view of the apparatus used for the presentation of visual stimuli.

of 1600 × 1200 with a pixel size of 0.24mm × 0.24 mm and a frame rate of 80 Hz. The graphics card allowed luminances to be specified with a resolution of 8 bits per gun. With a Photo Research PR-715 SpectraScan spectroradiometer, spectral emission functions were calibrated, the luminances of digital inputs were obtained through look-up tables (LUT). At the same time, for more accurate transformation between monitor RGB values and CIE XYZ, the effect of the black point was considered [26]. In our experiment, the CIE XYZ of the black point of the monitor were 0.221/0.284/0.333, the CIE 1931 chromaticity (x, y) of the white point was (0.314, 0.334), and the chromaticity (x, y) of the phosphors were (0.615, 0.344) for the red channel, (0.278, 0.605) for the green, and (0.150, 0.074) for the blue.

In a dark room, observers viewed the stimuli via a custom-built 4-mirror stereoscope with a viewing distance of 650 mm from the monitor screen, as shown in Fig. 1. The stereoscope permitted the left half and right half images of the screen to be projected to the left and right eyes, respectively, resulting in binocular viewing. In these conditions, the screen subtended 33.6° × 25.2° and each pixel subtended by about 1.2 arc minutes from the observation point.

B. STIMULI

The stimuli presented on the screen for the right and left eyes were generated and controlled by specially written software in C++. As shown in Fig. 2, the stimuli consist of a pair of 2° diameter circular patches for the left eye and the right eye on a black background with the luminance of 0.28 cd/m^2. In the CIE 1976 uniform chromaticity scale diagram, the color gamut of the CRT display can be represented by a triangle between red: u'v'(0.42, 0.53), green: u'v'(0.11, 0.56), and blue u'v'(0.17, 0.19). Five sample points within the color gamut of the monitor were selected to measure the color fusion limit, as shown in Fig. 3(a).

The right circular patch was filled with the sample point color and presented for the right eye, and the left circular patches were filled with neighbor point colors and presented for the left eye. Neighbor point colors were selected along the straight lines of six directions for the sample point color, as shown in Fig. 3(b). The six directions were three main directions to the red (R), green (G), and blue (B) primaries and three sub-directions representing an equiangular division between R and G, G and B, plus B and R, respectively. The neighbor points along each line increased the distance with a step size of 0.02 $\Delta E_{u'v'}$ from each sample point. Due to the limit of the display color gamut, the six directions did not select for all sample points and the number of neighbor points along each line was not the same, depending on the situation. For example, Fig. 3(b) shows the neighbor point selection scheme for the sample point No. 1, and the points on R-G and G-B directions were in the fusion range and not used to measure limits. A total of 184 neighbor points were selected for five sample points. Appendix Tables 3-5 list the u'v' values of all the selected points. Constrained at a luminance level of 10 cd/m^2, and first, the u'v' values of all selected points transformed to RGB values by an inverse process of the monitor characterization. Then, using the PR-715 spectroradiometer, the luminance and chromaticity of output for RGB values on the CRT monitor were measured at the center point of the screen. The color errors between the transformed and measured values of all points were extremely small, and the maximum color difference was 0.003 $\Delta E_{u'v'}$.

To measure the color fusion limit for different disparities, the left and right circular patches were horizontally adjusted on image pixels. There are two kinds of disparities: crossed disparity (where the object appears closer to the observer) and

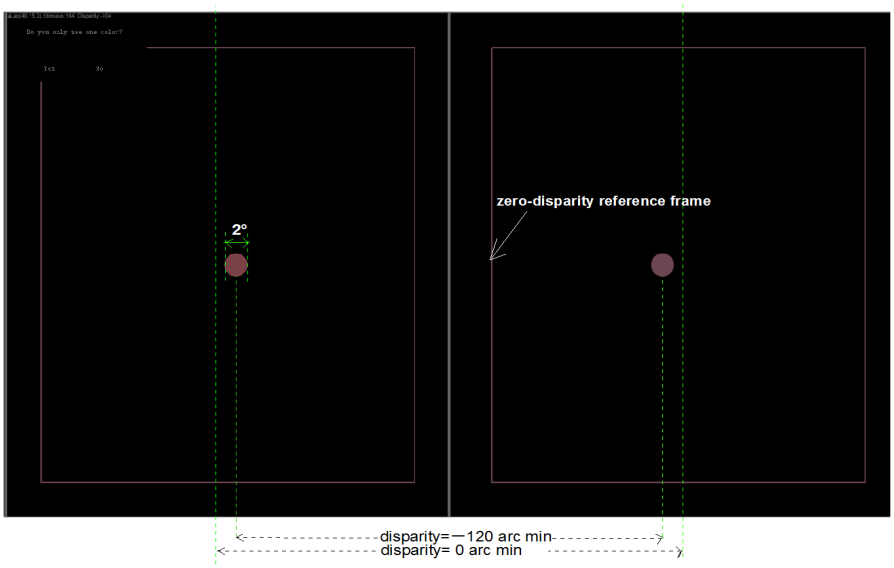

FIGURE 2. Illustration of visual stimulus with crossed disparity.

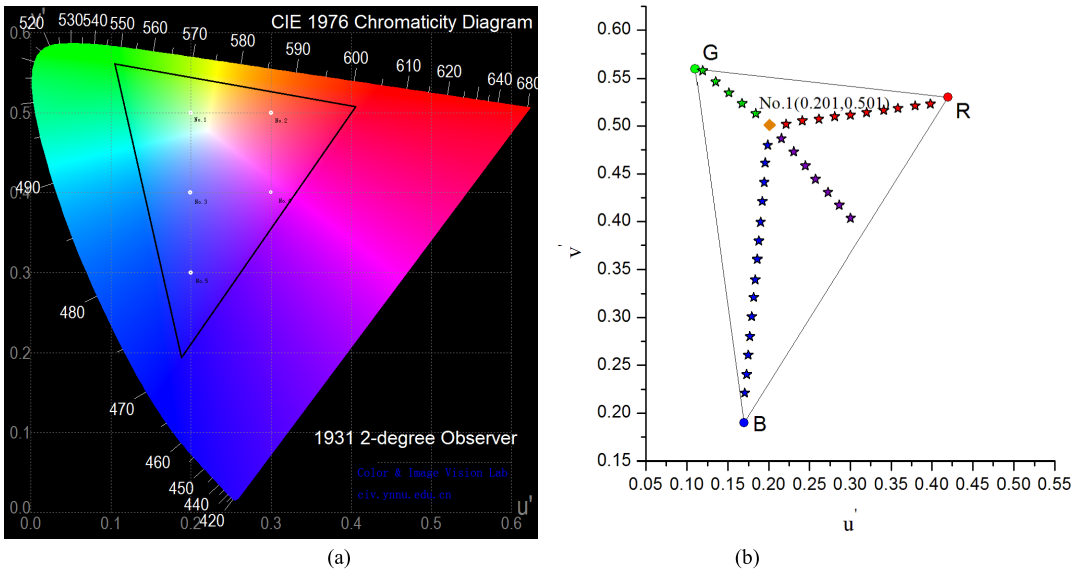

(a) (b)

FIGURE 3. Selection of color points: (a) five sample color points; (b) the neighbor points selection scheme for the sample point No. 1.

uncrossed disparity (where the object appears farther from the observer). To avoid the viewer simply making a vergence eye movement to view the binocular target and thereby having the absolute disparity zero in every case, a frame with the sample color serves as a zero-disparity reference, as shown in Fig. 2. For brief stimulus duration, disparity fusion limit can be as small as 24 arc minutes, but with longer stimulus durations and convergence eye movements, disparities can be as large as 4.93 degrees [27]. Here, five levels of relative screen disparity (i.e., the angular distance between two corresponding pixels in two separate views on the display) were given to the stimuli in the range of −120 to +120 arc minutes with a step size of 60 arc minutes, where negative polarity refers to crossed disparity while positive polarity refers to uncrossed disparity. The range of disparity had been determined in order for the color fusion limit to cover all possible range of binocular fusion in real stereoscopic images. Consequently, there were five disparity levels, which were ±120, ±60 and 0 arc minutes, and a total number of 920(= 184×5) stimuli were used.

C. OBSERVER

As the literature [14], we recruited two observers taking part in the experiment. One is HDY, male, 24 years old.

One is LLS, female, 23 years old. They all had normal color vision (Dvorine Color Plates, 2nd ed.) and normal stereoscopic acuity (stereo-fly tests). They were not aware of the purpose of the experiment and were all non-experts, in that their normal jobs did not concern stereoscopic graphics. No other exclusion criteria were applied. The experiment conformed to the standards set by the Declaration of Helsinki [28]. They read and signed informed consents, and were free to leave the study at any stage.

D. PROCEDURE

The experimental procedure was wholly controlled by the software. First, one kind of color was randomly selected from five sample colors to fill the circular patch on the right half screen. Then, the left circular patch was randomly filled with a neighbor color. And then a disparity level was randomly selected from five disparities to move the left and right circular patches horizontally on image pixels. For example, if the disparity was −120 arc minutes, the right patch was shifted to the left with 50 pixels, and the left patch was shifted to the right with 50 pixels, as shown in Fig. 2 (b). After the stimulus was generated, it was immediately displayed on the screen. The exposure time of the stimulus was 15 s, which was long enough to allow the observer to determine whether the two colors can be fused. The prompt of fusion or not was ''Do you only see one color?''. It was a forced choice. If the observer pressed the keyboard ''Y'' key, it meant that the brain could fuse the two colors. If the observer pressed the keyboard ''N'' key, it meant that the brain could not fuse the two colors. This information was automatically recorded in a program document after each sample color and all its surrounding neighbor colors were traversed for all disparity levels. This trial was repeated 10 times.

Therefore, a total of 9200 (i.e. 920 stimuli × 10 observations) trials were recorded for a single observer. The observation process for all of the trials was lengthy and induced visual fatigue. Thus, the observations were divided into several tests consisting of several 30-min sessions. The observations were stopped immediately when the observer sensed any visual fatigue.

III. RESULTS AND DISCUSSION

A. CALCULATION OF COLOR FUSION LIMIT

We recorded the number of responses with fusion for the 920 stimuli. At different disparity levels, the overall results of the fusion probability derived from the observations by two observers are presented in Tables 3–5 in the Appendix. The fusion probability ($p\%$) was calculated as follows:

$$p = \frac{Total\ number\ of\ responses\ with\ fusion}{Total\ number\ of responses\ with\ (fusion + nonfusion)} \times 100\% \quad (1)$$

where *Total number of responses with fusion* is the sum of the two observers' numbers, *Total number of responses with (fusion + nonfusion)* is 20 here. If a neighbor color had the 50% fusion probability, the Euclidean distance $\Delta E_{u'v'}$ from the corresponding sample point to this neighbor point was just selected as the color fusion limit.

In the literature [14], the color fusion limits of each sample point for different directions were calculated by using a linear interpolation formula. Using the interpolation method, however, it would not work when p(%) never exceeded 50%. Here, we used a psychometric function to fit curves of fusion probability [29]:

$$p(x) = \sum_{n=0}^{N} a_n (\ln x)^n \quad (2)$$

where $p(x)$ denotes the fusion probability for the neighbors in a line of the direction sampled for the left eye, x is the Euclidean distance from the sample color to the neighbor color; the basic function $\ln x$ represents that fusion probability takes the Weber-Fechner's law as the foundation; the power series of lnx represent that fusion probability is characterized as multi-items scales; there is a total of $N + 1$ items; and a_n represents the coefficient of the nth item, which could be obtained by fitting the psychometric function. By setting the different N, regression analysis was performed to find the optimal value of the coefficient a_n, and the coefficient of determination – R^2 values were examined for the goodness-of-fit statistics of the regressions. Table 1 lists the values of R^2 with N variations regarding the left stimuli sampled in red (R) direction from the No. 1 point ($u' = 0.20$, $v' = 0.50$). As it is seen from Table 1, R^2 close to 1 when N increases. In Table 1, when $N = 3$, the values R^2 are bigger than 0.95. Accordingly, we selected $N = 3$ for all regression analyses. Figure 4 shows the fusion probability of the No. 1 color point in red (R) direction at different disparities. The abscissa represents the Euclidean distance from the point in the u' v' chromaticity diagram. Once the psychometric function - Eq. (2) has been fitted, the color fusion limit $\Delta E_{u'v'}$ was obtained by setting $p(x) = 50$, as presented in Tables 3-5 in the Appendix.

B. RESULTS OF COLOR FUSION LIMIT

Fig. 5 shows the fusion limit scatters of five sample color points for different disparities along different color directions by using data in Appendix Table 3-5. As it can be seen, there were different fusion limits at different levels of disparity for all of the sample points. The average values of the fusion limits for different disparities are listed in the bottom of Appendix Table 5, and the average fusion limit increases as the disparity varies from −120 to +120 arc minutes. The minimum of fusion limit is 0.036 $\Delta E_{u'v'}$ when the disparity is −120 arc minutes, and the maximum of fusion limit is 0.064 $\Delta E_{u'v'}$ when the disparity is +120 arc minutes. The fusion limits present a gradation, and the means are significantly different ($F(4, 100) = 7.53, p < 0.01$) at the significance level 0.05. In addition, there are different fusion limits on color directions for all of the sample points. For example, the sample point No. 3 has the maximum fusion limit of 0.051 $\Delta E_{u'v'}$ on the direction G and has the minimum

TABLE 1. The performances of regression analysis: values of R^2 for different$N$. (d denotes disparity).

N	R^2				
	d=-120'	d=-60'	d=0'	d=+60'	d=+120'
1	0.8854	0.9389	0.8939	0.9027	0.9762
2	0.9521	0.9478	0.9157	0.9106	0.9766
3	0.9571	0.9893	0.9620	0.9517	0.9832
4	0.9572	0.9935	0.9900	0.9782	0.9867

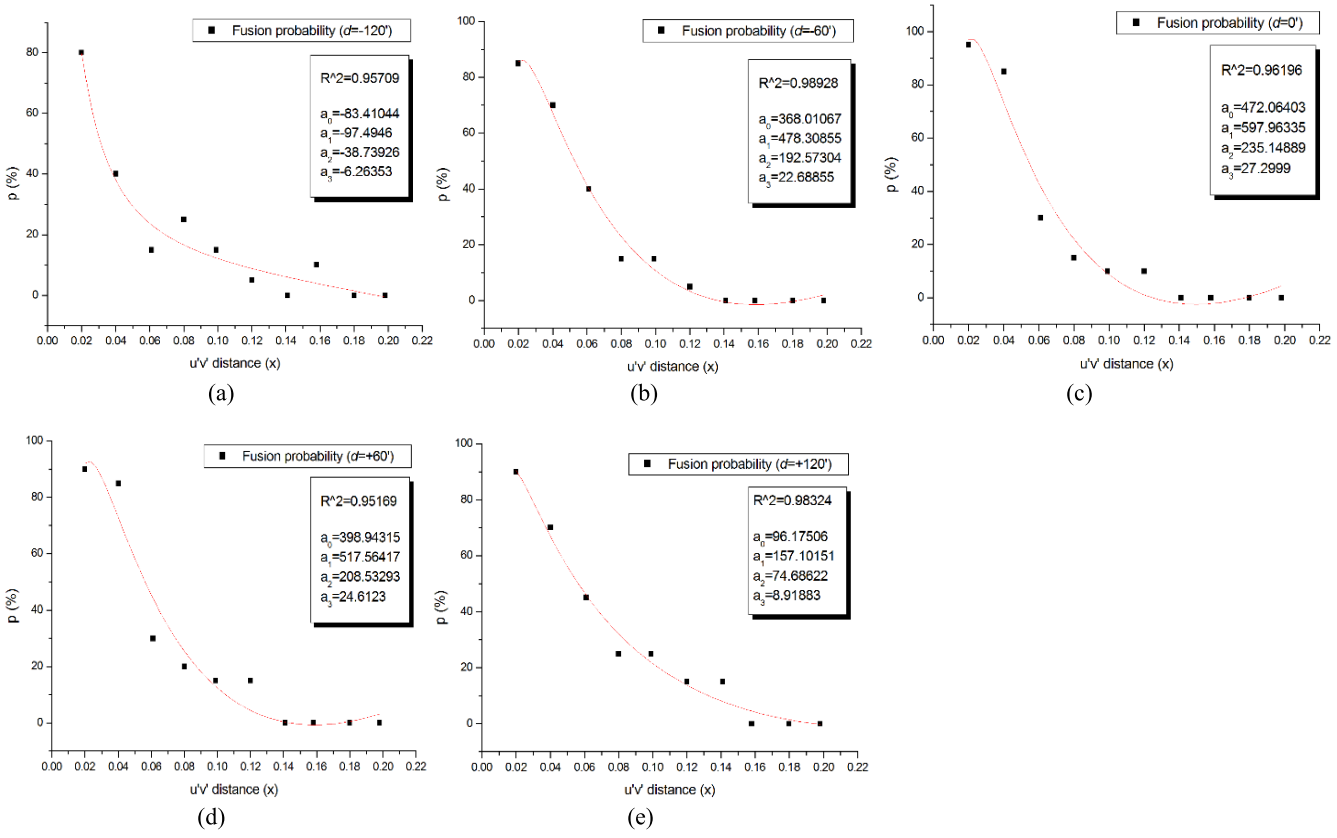

FIGURE 4. The fusion probability of sample point No.1 (0.2, 0.5) on direction R at different disparities d: (a) d = −120′, (b) d = −60′, (c) d = 0′, (d) d = +60′, and (e) d = +120′.

fusion limit of 0.019 $\Delta E_{u'v'}$ on the direction B at the level of disparity −120′ .

1) EFFECT OF DISPARITY SIGN ON COLOR FUSION LIMIT

Fig. 6 presents the curve shape of color fusion limits averaged over the sample points as a function of the disparity. As it is seen in fig. 6, the disparity sign also has an impact on the color fusion limit. For the crossed disparity (−), the fusion limit increases as the disparity decreases. But for the uncrossed disparity (+), the fusion limit increases as the disparity increases. This is contrary to our expectations, because, in a sense, to increase the disparity information is to increase the burden of the human eye, fusion limit should be reduced accordingly, just like Qin et al.'s the results [15], which showed that the fusion limit became smaller as the stimulation brightness increased. This seems to explain that the human eye has different information processing mechanisms for the crossed disparity and the uncrossed disparity, and the uncrossed disparity may contribute to color fusion. The uncrossed disparity may also cause the observation target going away from the viewer so that the observer cannot determine the color fusion clearly. Instead, crossed disparity makes the target close the observer, and the observer can thus be made more sensitive to the color identification, leading to fusion limit decreases. Usually, we think that color vision is a lowlevel monocular vision, while stereo vision is a high-level binocular vision, so the influence of color information on binocular disparity fusion is positive [21], [22], [30]. But we have shown here that the binocular disparity fusion would also affect the color fusion. In short, the phenomenon that

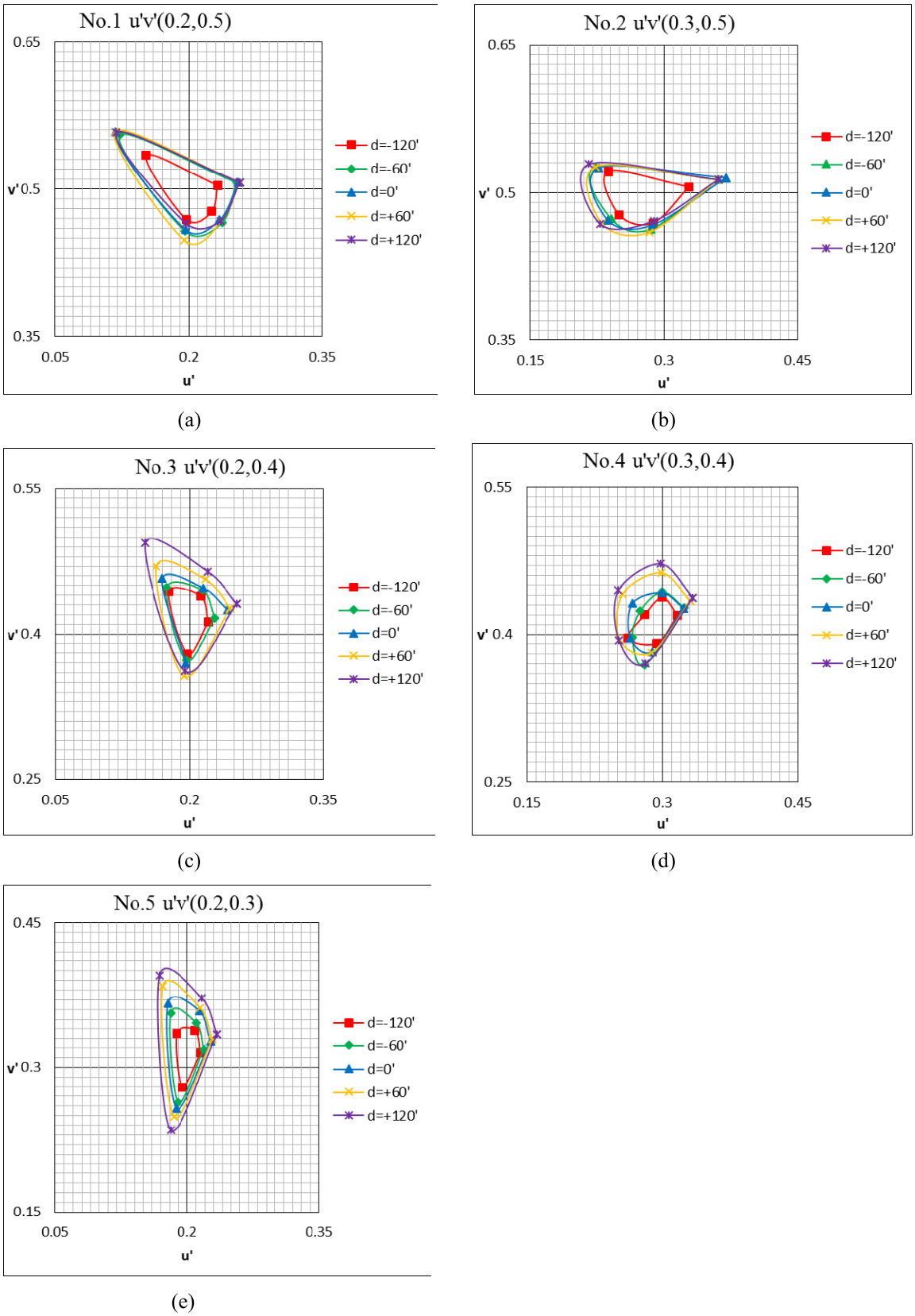

FIGURE 5. Fusion limit scatters for each of the sample color points in Fig. 3: (a) No.1 point ($u' = 0.2$, $v' = 0.5$), (b) No.2 point ($u' = 0.3$, $v' = 0.5$), (c) No.3 point ($u' = 0.2$, $v' = 0.4$), (d) No.4 point ($u' = 0.3$, $v' = 0.4$), and (e) No.4 point ($u' = 0.3$, $v' = 0.4$). The fusion limit was marked along each color direction line for different disparities.

TABLE 2. Estimated parameter values of ellipses for five sample color points at different disparities.

Sample point (u′, v′)	parameter	d=-120'	d=-60'	d=0'	d=+60'	d=+ 120'
No.1 (0.2,0.5)	a	0.054	0.090	0.099	0.094	0.121
	b	0.027	0.038	0.037	0.046	0.032
	θ(rad)	21.324	21.476	21.515	21.370	21.603
No.2 (0.3,0.5)	a	0.069	0.084	0.092	0.087	0.115
	b	0.034	0.041	0.036	0.045	0.036
	θ(rad)	9.295	9.273	9.388	9.372	9.390
No.3 (0.2,0.4)	a	0.054	0.055	0.086	0.091	0.145
	b	0.024	0.033	0.045	0.051	0.059
	θ(rad)	-20.176	-20.081	-19.358	-19.523	-19.507
No.4 (0.3,0.4)	a	0.036	0.042	0.048	0.067	0.079
	b	0.033	0.032	0.033	0.044	0.045
	θ(rad)	-9.880	-11.003	-10.377	-10.521	-10.574
No.5 (0.2,0.3)	a	0.045	0.066	0.073	0.090	0.102
	b	0.017	0.022	0.032	0.036	0.042
	θ(rad)	-20.365	-20.260	-20.234	-20.161	-20.185

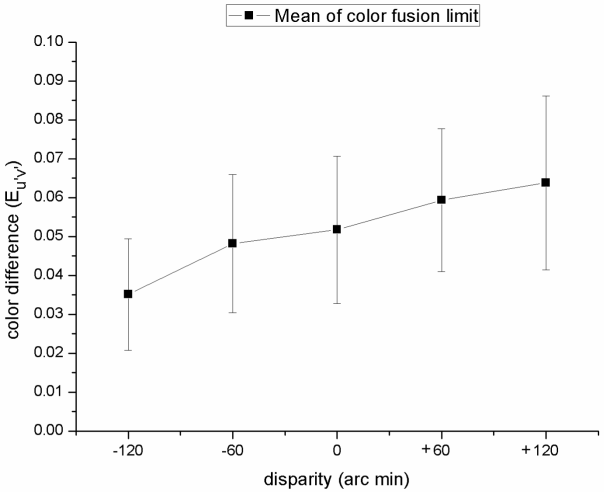

FIGURE 6. The color fusion limit as a function of the disparity. The error bar represents 95% confidence interval.

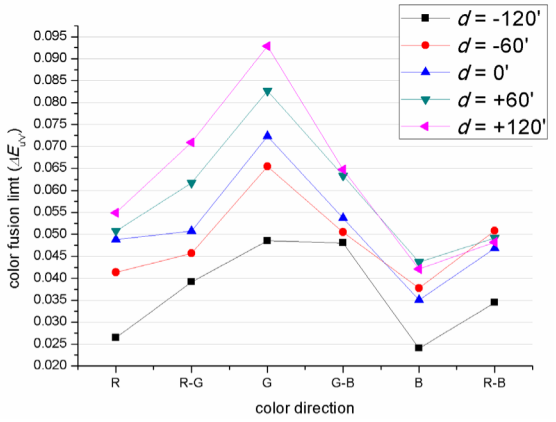

FIGURE 7. The color fusion limits on different color directions at different disparity levels. *d* indicates the disparity.

stereo vision affects color vision deserves more experiments to be discussed.

2) EFFECT OF COLOR DIRECTION ON COLOR FUSION LIMIT

As can be seen from Fig 5, the color fusion limits are not equal on each color direction in the standard uniform chromaticity diagram. For comparative purpose, we computed the color fusion limit for each color direction by averaging over the sample points. Fig. 7 shows the relation between color fusion limit and color direction at given disparity magnitudes. From Fig.7, it can be seen that the color fusion limit has a gradation on different color directions. We can clearly see that the color fusion limit on green (G) direction is the largest, and the color fusion limit on blue (G) direction is the smallest for every disparity magnitude. In a previous study. we reported that the disparity fusion range varied with the hues [22]. We found that the green random-dot stereogram (RDS) stimuli were the most difficult to fuse and perceive its depth in 3D displays. The result of this study also shows the subject eyes are insensitive to the green hue, resulting in a large color fusion limit on green direction. According to literature, the red- and green-sensitive cones make up more than about 90% of the total cones in the retina [31], and blue cones only constitute 10% of all cones and are always surrounded by longer-wavelength cones [32]. Wilson *et al.* [33] found that the maximum disparity that could be fused was the same for the blue cones as for the entire visual system, and confirmed that color stereoscopic perception has nothing to do with the distribution of cone cells. The experimental results here indicate that the color fusion limit varies with the color direction, but it has nothing to do with the distribution of cone cells.

C. QUANTIFICATION OF COLOR FUSION LIMIT

About expressions of color fusion limit, Ikeda and Sagawa [5] and Qin *et al.* [15], who studied the spectral colors,

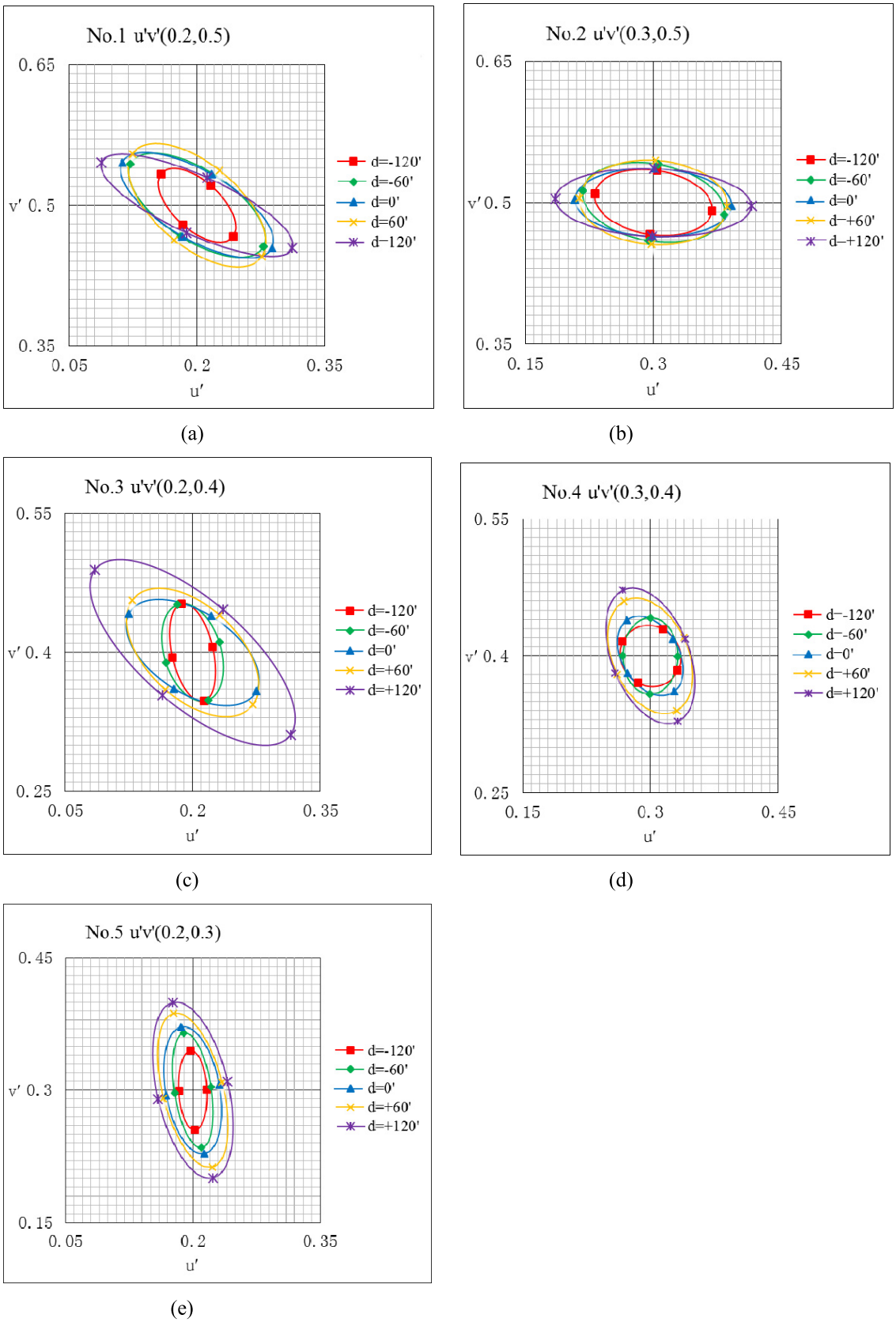

FIGURE 8. Quantified ellipses of fusion limits for each of the sample color points at different levels of disparity. (a) No.1 point ($u' = 0.2$, $v' = 0.5$), (b) No.2 point ($u' = 0.3$, $v' = 0.5$), (c) No.3 point ($u' = 0.2$, $v' = 0.4$), (d) No.4 point ($u' = 0.3$, $v' = 0.4$), and (e) No.4 point ($u' = 0.3$, $v' = 0.4$).

TABLE 3. The selection of sample points and neighbor points, the percentage of fusion rates and the fusion limits. p(%) indicates fusion probability at different disparities; $\Delta E_{u'v'}$ indicates color fusion limit (the distance of color difference); L indicates the straight lines of the directions from sample points; and is the Euclidean distance from the sample color to the neighbor color.

sample point	neighbor point				p(%)					$\Delta E_{u'v'}$				
(u′,v′)	L	u′	v′	x	-120'	-60'	0'	+60'	+120'	-120'	-60'	0'	+60'	+120'
No.1 (0.2,0.5)	R	0.221	0.502	0.020	80	85	95	90	90	0.031	0.053	0.055	0.056	0.056
		0.241	0.506	0.040	40	70	85	85	70					
		0.261	0.507	0.061	15	40	30	30	45					
		0.281	0.510	0.080	25	15	15	20	25					
		0.300	0.511	0.099	15	15	10	15	25					
		0.320	0.514	0.120	5	5	10	15	15					
		0.341	0.517	0.141	0	0	0	0	15					
		0.358	0.519	0.158	10	0	0	0	0					
		0.379	0.521	0.180	0	0	0	0	0					
		0.398	0.523	0.198	0	0	0	0	0					
	G	0.184	0.513	0.021	95	95	95	90	100	0.059	0.095	0.101	0.102	0.100
		0.167	0.524	0.041	65	80	95	100	100					
		0.151	0.535	0.060	45	60	85	85	100					
		0.135	0.546	0.080	50	65	75	80	80					
		0.119	0.558	0.100	45	45	50	50	50					
	B	0.199	0.480	0.021	70	80	95	85	90	0.033	0.045	0.043	0.054	0.036
		0.196	0.462	0.040	35	45	45	50	50					
		0.194	0.441	0.061	40	40	40	50	30					
		0.192	0.421	0.081	40	50	40	40	20					
		0.190	0.399	0.103	30	40	30	40	35					
		0.188	0.380	0.122	25	30	30	25	25					
		0.186	0.361	0.141	20	30	25	15	40					
		0.183	0.340	0.163	15	25	10	5	20					
		0.181	0.321	0.181	20	0	10	10	15					
		0.179	0.301	0.201	10	10	15	10	20					
		0.177	0.280	0.222	5	10	10	5	25					
		0.175	0.261	0.242	15	10	10	5	25					
		0.173	0.241	0.262	5	0	0	5	15					
		0.171	0.221	0.282	0	0	5	0	15					
	R-B	0.215	0.487	0.020	60	100	95	100	85	0.034	0.051	0.047	0.049	0.048
		0.231	0.473	0.041	45	60	55	65	60					
		0.245	0.458	0.061	35	40	40	25	35					
		0.257	0.444	0.080	25	35	25	40	30					
		0.273	0.431	0.100	20	10	25	5	10					
		0.287	0.417	0.120	10	10	0	15	25					
		0.300	0.404	0.139	10	5	10	5	5					
No.2 (0.3,0.5)	R	0.321	0.505	0.019	70	85	95	90	85	0.026	0.060	0.069	0.059	0.060
		0.341	0.508	0.039	35	60	75	75	95					
		0.360	0.514	0.059	15	60	70	65	65					
		0.378	0.517	0.077	20	25	30	10	10					
		0.399	0.522	0.098	5	10	0	0	15					
	G	0.283	0.508	0.021	85	85	95	100	95	0.069	0.083	0.080	0.083	0.091
		0.264	0.513	0.040	85	80	95	100	95					
		0.246	0.518	0.060	50	60	60	55	65					
		0.225	0.525	0.081	35	50	45	50	50					
		0.207	0.532	0.100	40	40	35	45	45					
		0.187	0.538	0.121	30	50	45	45	50					
		0.168	0.544	0.142	35	30	45	35	50					
		0.148	0.551	0.162	40	40	45	35	50					
		0.130	0.556	0.181	30	35	40	40	50					
	B	0.295	0.482	0.020	80	85	85	90	80	0.035	0.042	0.037	0.045	0.033
		0.285	0.465	0.040	40	40	40	50	40					
		0.277	0.446	0.060	40	50	45	45	35					
		0.270	0.429	0.079	50	40	35	35	40					
		0.262	0.409	0.100	30	25	25	20	40					
		0.254	0.391	0.119	35	30	30	30	25					
		0.246	0.372	0.140	20	20	15	15	25					
		0.239	0.353	0.161	25	5	20	10	15					
		0.230	0.334	0.182	5	15	5	10	25					
		0.222	0.316	0.202	10	10	0	0	5					
		0.214	0.297	0.222	0	5	0	5	10					
		0.206	0.279	0.242	0	5	0	0	5					

TABLE 4. Continued table 3.

sample point	neighbor point				p(%)					$\Delta E_{u'v'}$				
(u′,v′)	L	u′	v′	χ	-120'	-60'	0'	+60'	+120'	-120'	-60'	0'	+60'	+120'
No.2 (0.3,0.5)	G-B	0.284	0.492	0.020	85	95	100	95	95	0.058	0.067	0.071	0.079	0.081
		0.264	0.485	0.041	65	95	90	100	90					
		0.247	0.475	0.061	45	40	60	60	50					
		0.228	0.468	0.081	35	40	35	50	45					
		0.210	0.459	0.101	25	20	25	30	40					
		0.191	0.451	0.122	25	20	25	20	40					
		0.173	0.443	0.142	20	15	10	25	30					
		0.155	0.433	0.162	0	10	0	10	25					
		0.136	0.427	0.182	0	0	5	5	10					
No.3 (0.2,0.4)	R	0.217	0.409	0.020	65	75	80	90	80	0.024	0.033	0.049	0.053	0.061
		0.235	0.421	0.041	20	45	75	85	75					
		0.253	0.433	0.062	15	15	20	20	40					
		0.270	0.441	0.081	5	10	10	10	30					
		0.287	0.451	0.101	10	5	5	10	35					
		0.306	0.460	0.122	0	5	0	0	25					
		0.322	0.471	0.141	0	10	10	10	20					
		0.339	0.481	0.161	0	0	0	0	20					
		0.356	0.491	0.180	0	5	0	5	5					
		0.374	0.502	0.201	0	0	0	5	0					
	G	0.191	0.417	0.021	80	90	80	90	80	0.051	0.056	0.067	0.081	0.108
		0.182	0.436	0.042	65	75	75	85	90					
		0.172	0.453	0.062	35	35	65	80	75					
		0.162	0.472	0.083	30	30	35	35	60					
		0.153	0.490	0.104	25	15	15	40	50					
		0.143	0.508	0.124	35	15	25	40	50					
		0.134	0.525	0.143	20	10	20	20	40					
		0.125	0.541	0.162	20	25	25	35	35					
	B	0.198	0.379	0.020	50	65	75	85	95	0.019	0.026	0.029	0.043	0.037
		0.194	0.360	0.039	10	35	40	50	45					
		0.191	0.341	0.058	30	30	40	50	50					
		0.188	0.319	0.080	40	40	40	35	45					
		0.185	0.299	0.101	20	20	40	30	35					
		0.182	0.281	0.119	20	15	30	40	45					
		0.179	0.261	0.139	25	15	20	30	45					
		0.176	0.241	0.160	15	20	20	20	45					
		0.173	0.222	0.179	10	10	10	20	30					
		0.170	0.202	0.199	10	5	0	15	30					
	R-G	0.207	0.420	0.022	80	80	80	90	90	0.042	0.049	0.051	0.060	0.069
		0.212	0.439	0.042	60	60	60	85	75					
		0.218	0.459	0.063	15	30	45	45	65					
		0.223	0.478	0.082	5	20	10	15	25					
		0.229	0.496	0.102	25	5	10	10	30					
		0.234	0.516	0.122	0	0	10	5	20					
		0.241	0.535	0.142	10	0	5	5	5					
		0.244	0.553	0.160	0	0	0	0	0					
No.4 (0.3,0.4)	R	0.315	0.418	0.022	55	75	85	85	80	0.024	0.035	0.034	0.045	0.049
		0.328	0.432	0.041	25	45	40	60	65					
		0.341	0.446	0.060	20	15	20	25	30					
		0.354	0.459	0.079	0	10	15	15	20					
		0.368	0.475	0.100	5	10	10	10	20					
		0.383	0.489	0.121	5	0	0	10	0					
		0.396	0.503	0.140	0	0	0	0	0					
	G	0.287	0.415	0.019	55	60	75	80	90	0.027	0.033	0.045	0.059	0.065
		0.272	0.429	0.039	40	50	65	75	75					
		0.255	0.440	0.059	25	30	25	45	50					
		0.240	0.453	0.079	10	15	25	35	40					
		0.227	0.466	0.097	10	25	20	20	40					
		0.210	0.479	0.119	10	5	20	25	40					
		0.195	0.493	0.139	10	25	20	35	45					
		0.179	0.505	0.159	10	20	0	20	45					
		0.164	0.519	0.180	10	5	15	10	45					

TABLE 5. Continued table 4.

sample point	neighbor point				p(%)					$\Delta E_{u'v'}$				
(u′,v′)	L	u′	v′	x	-120'	-60'	0'	+60'	+120'	-120'	-60'	0'	+60'	+120'
No.4 (0.3,0.4)	B	0.290	0.385	0.020	40	55	55	55	55	0.012	0.038	0.023	0.023	0.037
		0.280	0.368	0.039	30	50	35	40	45					
		0.269	0.351	0.060	35	35	30	35	45					
		0.259	0.334	0.079	20	30	20	25	40					
		0.248	0.316	0.101	25	15	20	25	25					
		0.236	0.298	0.122	20	5	15	20	30					
		0.226	0.281	0.142	5	15	5	20	15					
		0.215	0.264	0.161	0	10	5	5	15					
		0.205	0.247	0.181	5	0	0	5	20					
	R-G	0.301	0.423	0.021	65	80	90	90	90	0.036	0.042	0.041	0.061	0.070
		0.299	0.440	0.038	55	60	60	85	75					
		0.298	0.461	0.060	10	20	25	35	45					
		0.298	0.482	0.081	15	10	15	40	45					
		0.297	0.501	0.099	10	5	30	20	35					
		0.295	0.521	0.119	10	15	15	35	30					
		0.293	0.539	0.137	0	0	0	0	0					
	G-B	0.282	0.399	0.018	65	80	85	80	95	0.039	0.034	0.036	0.048	0.049
		0.262	0.396	0.038	45	45	45	70	60					
		0.242	0.393	0.059	40	30	30	30	40					
		0.222	0.389	0.079	15	15	20	15	40					
		0.202	0.386	0.100	0	25	5	15	35					
		0.181	0.381	0.120	5	0	5	20	25					
		0.162	0.377	0.140	0	0	0	5	25					
		0.142	0.375	0.160	0	0	0	0	20					
No.5 (0.2,0.3)	R	0.214	0.314	0.020	55	60	80	80	90	0.0212	0.026	0.037	0.040	0.048
		0.228	0.328	0.040	20	35	50	55	60					
		0.241	0.343	0.059	10	25	25	30	40					
		0.256	0.358	0.081	15	10	15	20	30					
		0.271	0.374	0.102	10	10	15	25	30					
		0.284	0.388	0.121	5	5	5	10	15					
		0.298	0.404	0.143	0	5	0	5	20					
		0.312	0.418	0.162	0	0	0	5	5					
		0.326	0.432	0.182	0	0	0	0	0					
		0.340	0.447	0.203	0	0	0	0	0					
	G	0.194	0.317	0.018	80	95	85	80	100	0.037	0.059	0.070	0.089	0.100
		0.188	0.336	0.038	60	75	95	100	90					
		0.181	0.357	0.059	25	40	60	80	80					
		0.175	0.375	0.078	15	20	40	45	50					
		0.169	0.396	0.100	25	15	20	25	40					
		0.163	0.413	0.118	20	25	10	35	40					
		0.156	0.434	0.141	20	5	15	35	45					
		0.150	0.452	0.159	10	5	0	35	45					
		0.144	0.473	0.181	15	5	15	15	35					
		0.138	0.491	0.201	5	5	5	15	30					
		0.131	0.510	0.221	10	0	5	10	35					
		0.125	0.528	0.240	5	10	5	5	20					
	B	0.194	0.280	0.021	50	65	85	90	90	0.021	0.038	0.044	0.054	0.068
		0.189	0.261	0.041	35	45	55	65	70					
		0.183	0.242	0.061	40	35	30	45	50					
		0.178	0.223	0.081	20	20	25	30	50					
		0.172	0.204	0.101	10	30	20	30	45					
	R-G	0.205	0.319	0.019	60	85	85	95	90	0.040	0.047	0.060	0.064	0.073
		0.209	0.338	0.039	60	65	85	90	95					
		0.214	0.358	0.060	20	30	45	50	60					
		0.219	0.378	0.080	30	20	30	30	35					
		0.223	0.399	0.101	5	15	10	15	30					
		0.227	0.418	0.121	15	15	5	5	25					
		0.232	0.438	0.141	15	5	0	20	10					
		0.237	0.458	0.162	0	0	0	5	20					
		0.241	0.475	0.180	0	0	5	5	5					
		0.246	0.495	0.200	0	5	0	0	0					
Mean										0.036	0.048	0.052	0.059	0.064

used $\Delta\lambda$ to indicate the fusion limit for the wavelength λ. For non-spectral color, Ikeda et al. [13] used a circle to represent the fusion limit of the white light. However, Jung et al. considered that the shape of the chromaticity points of the color fusion limit could be more accurately represented by ellipses [14]. The elliptic equation is defined as:

$$\frac{[(u'-\mathrm{u}'_0)\cos\theta+(v'-\mathrm{v}'_0)\sin\theta]^2}{\mathrm{a}^2}+\frac{[-(u'-\mathrm{u}'_0)\sin\theta+(v'-\mathrm{v}'_0)\cos\theta]^2}{\mathrm{b}^2}=1 \quad (3)$$

where u' and v' denote the fusion limit point for sample point(u'_0, v'_0); θ is the rotation angle of the ellipse; a and b are the semi-major and semi-minor axes from the sample point(u'_0, v'_0), respectively. Based on equation (3), regression analysis was performed to find the optimal parameters of the ellipse. Fig. 8 represents ellipses that quantify the color fusion limit for each sample color point at different disparity levels. All of the ellipses are plotted on the same scale. Table 2 summarizes the estimated parameter values of the ellipses for the five sample points. The semi-minor axis a ranges from 0.036 to 0.145 $\Delta E_{\mathrm{u'v'}}$, whereas the semi-major axis b ranges from 0.017 to 0.059 $\Delta_{u'v'}$. The average of the a values is 0.079 $\Delta E_{\mathrm{u'v'}}$ and the average of the b values is 0.037 $\Delta E_{\mathrm{u'v'}}$. From Fig. 8, it can be seen that the rotation angle of the ellipses is basically consistent at different disparities, except for point No.3.

D. SAFETY OF BINOCULAR COLOR FUSION

It is also worth noting that visual discomfort appeared during the experiment. To quantify the color fusion limit, we had to obtain more accurate information by examining more stimuli. For an observer, the number of observations became very large. The observers reported that the visually uncomfortable feeling was strong when the color difference of two eyes was significantly increased, though the binocular color fusion could occur without color rivalry. Qin et al. suggested that only when the color difference of the irritant light between right-and-left eyes was smaller than the color fusion limit, an even and stable image in the visual field could be obtained [17]. In 3D content creation and 3D system design process, however, only to ensure that the color difference within the fusion limit range is not enough, you need to have more stringent standards, which the color difference between the left and right eyes should be within a comfortable range. In previous work, we recommended that color difference should not exceed 0.019 $\Delta E_{\mathrm{u'v'}}$ between the stereo image pairs [34]. As long as the color difference between two eyes exceeds this threshold, even if the color rivalry does not occur, it will easily lead to visual discomfort.

IV. CONCLUSIONS

In this paper, we measured the binocular color fusion limit for different binocular disparities. The color fusion limits were obtained for five chromaticity points sampled from the 1976 CIE u'v' chromaticity diagram. The experimental results showed that there were multi-factors influencing the color fusion limit for each sample color point. Each color point had a different fusion limit on each color direction, and the fusion limit was not the same for different disparity levels. The color fusion limit quantified by ellipses ranges from 0.017 to 0.145 $\Delta E_{\mathrm{u'v'}}$ for the disparities from -120 to $+120$ arc minutes. These quantitative experimental data confirmed that the binocular disparity fusion would also affect color fusion.

It was also worth noting that the disparity sign also had an impact on the color fusion limit. For the crossed disparity (sign $-$), the fusion limit increases as the disparity decreases. But for the uncrossed disparity (sign $+$), the fusion limit increases with the disparity increasing. In future work, the influences of disparity sign on the fusion limit need more experiments and studies to reveal its inner mechanism.

APPENDIX

See Tables 3–5.

REFERENCES

[1] N. Qian and A. Nieder, "Binocular disparity and the perception of depth," *Neuron*, vol. 18, pp. 359–368, Mar. 1997.
[2] Z. Chen, J. Shi, L. Yun, and Y. Tai, "A design of near-eye 3D display based on dual-OLED," *Proc. SPIE*, vol. 7749, Jul. 2010, Art. no. 774912.
[3] L. Liu, O. D. Vel, Q. L. Han, J. Zhang, and Y. Xiang, "Detecting and preventing cyber insider threats: A survey," *IEEE Commun. Surveys Tuts.*, vol. 20, no. 2, pp. 1397–1417, 2nd Quart., 2018.
[4] J. Chen, J. Zhou, J. Sun, and A. C. Bovik, "Binocular mismatch induced by luminance discrepancies on stereoscopic images," in *Proc. IEEE Int. Conf. Multimedia Expo*, Jul. 2014, pp. 1–6.
[5] M. Ikeda and K. Sagawa, "Binocular color fusion limit," *J. Opt. Soc. Amer.*, vol. 69, pp. 316–321, 1979.
[6] N. J. Wade and P. Wenderoth, "The influence of colour and contour rivalry on the magnitude of the tilt after-effect," *Vis. Res.*, vol. 18, no. 7, pp. 827–835, 1978.
[7] J. K. Hovis, "Review of dichoptic color mixing," *Optometry Vis. Sci.*, vol. 66, no. 3, pp. 181–190, 1989.
[8] N. Sun, J. Zhang, P. Rimba, S. Gao, Y. Xiang, and L. Y. Zhang, "Data-driven cybersecurity incident prediction: A survey," *IEEE Commun. Surveys Tuts.*, to be published.
[9] D. E. Johannsen, "A quantitative study of binocular color vision," *J. Gen. Psychol.*, vol. 4, nos. 1–4, pp. 282–308, 1930.
[10] R. W. Pickford, "Binocular colour combinations," *Nature*, vol. 159, pp. 268–269, Feb. 1947.
[11] L. M. Hurvich and D. Jameson, "The binocular fusion of yellow in relation to color theories," *Science*, 1951.
[12] I. Kovács, T. V. Papathomas, M. Yang, and Á. Fehér, "When the brain changes its mind: Interocular grouping during binocular rivalry," *Proc. Nat. Acad. Sci. USA*, vol. 93, no. 26, pp. 15508–15511, 1996.
[13] M. Ikeda and Y. Nakashima, "Wavelength difference limit for binocular color fusion," *Vis. Res.*, vol. 20, no. 8, pp. 693–697, 1980.
[14] Y. J. Jung, H. Sohn, S.-I. Lee, Y. M. Ro, and H. W. Park, "Quantitative measurement of binocular color fusion limit for non-spectral colors," *Opt. Express*, vol. 19, no. 8, pp. 7325–7338, 2011.
[15] D. Qin, M. Takamatsu, Y. Nakashima, and X. Qin, "Change of wavelength difference limit for binocular color fusion with wavelength and brightness of stimuli," *J. Light Vis. Environ.*, vol. 30, no. 1, pp. 43–45, 2006.
[16] X. Qin, Y. Nakashima, M. Takamatsu, and Y. Kidoh, "Research of binocular colour fusion limit on peripheral visual field," *J. Light Vis. Environ.*, vol. 31, no. 3, pp. 155–156, 2007.
[17] X. Qin, M. Takamatsu, and Y. Nakashima, "Effects of luminance and size of stimuli upon binocular color fusion limit," *Opt. Rev.*, vol. 16, pp. 404–408, May 2009.
[18] S. Y. Bae, R. Korniski, A. Ream, E. Fritz, and M. Shearn, "Single lens dual-aperture 3D imaging system: Color modeling," *Proc. SPIE*, vol. 8288, Feb. 2012, Art. no. 828807.

[19] F. L. Kooi and A. Toet, "Visual comfort of binocular and 3D displays," *Displays*, vol. 25, nos. 2–3, pp. 99–108, Aug. 2004.
[20] M. Lambooij, W. IJsselsteijn, M. Fortuin, and I. Heynderickx, "Visual discomfort and visual fatigue of stereoscopic displays: A review," *J. Imag. Sci. Technol.*, vol. 53, May 2009, Art. no. 030201.
[21] C. Lu and D. H. Fender, "The interaction of color and luminance in stereoscopic vision," *Investigative Ophthalmol.*, vol. 11, pp. 482–490, 1972.
[22] Z. Chen, J. Shi, Y. Tai, and L. Yun, "Stereoscopic depth perception varies with hues," *Opt. Eng.*, vol. 51, no. 9, 2012, Art. no. 097401.
[23] L. M. J. Meesters, W. A. IJsselsteijn, and P. J. H. Seuntiens, "A survey of perceptual evaluations and requirements of three-dimensional TV," *IEEE Trans. Circuits Syst. Video Technol.*, vol. 14, no. 3, pp. 381–391, Mar. 2004.
[24] J. Zhang, Y. Xiang, Y. Wang, W. Zhou, Y. Xiang, and Y. Guan, "Network traffic classification using correlation information," *IEEE Trans. Parallel Distrib. Syst.*, vol. 24, no. 1, pp. 104–117, Jan. 2013.
[25] Z. Chen, J. Shi, Y. Tai, X. Huang, and Z. Chao, "A quantitative measurement of binocular color fusion limit for different disparities," in *Proc. SPIE*, vol. 10616, Jan. 2018, Art. no. 1061604.
[26] J. Shi, L. Yun, J. Yan, H. Yu, and Y. Wang, "Accuracy of colorimetric characterization and effect of black point for CRT monitor," *Acta Opt. Sinica*, vol. 27, pp. 371–376, Feb. 2007.
[27] Y. Y. Yeh and L. D. Silverstein, "Limits of fusion and depth judgment in stereoscopic color displays," *Hum. Factors*, vol. 32, p. 45, 1990.
[28] WMA. *Ethical Principles for Medical Research Involving Human Subjects*. [Online]. Available: http://www.wma.net/en/30publications/10policies/b3/
[29] Z. Chen, J. Shi, X. Huang, L. Yun, and Y. Tai, "Visual comfort modeling for disparity in 3D contents based on Weber–Fechner's law," *J. Display Technol.*, vol. 10, pp. 1001–1009, Dec. 2014.
[30] S. Anstis and B. Rogers, "Binocular fusion of luminance, color, motion and flicker–two eyes are worse than one," *Vis. Res.*, vol. 53, pp. 47–53, Jan. 2012.
[31] K. C. Wikler and P. Rakic, "Distribution of photoreceptor subtypes in the retina of diurnal and nocturnal primates," *J. Neurosci.*, vol. 10, p. 3390, Oct. 1990.
[32] W. Li and S. H. DeVries, "Separate blue and green cone networks in the mammalian retina," *Nature Neurosci.*, vol. 7, pp. 751–756, Jun. 2004.
[33] H. R. Wilson, R. Blake, and J. Pokorny, "Limits of binocular fusion in the short wave sensitive ('blue') cones," *Vis. Res.*, vol. 28, no. 4, pp. 555–562, 1988.
[34] Z. Chen, X. Huang, Y. Tai, J. Shi, and L. Yun, "Visual discomfort caused by color asymmetry in 3D displays," *Pro. SPIE*, vol. 10022, Art. no. 100222T, Oct. 2016.